On the Numerical Modeling of Elastic Resonant Acoustic Scatterers

V. Romero-García*[1], A. Krynkin[2], J.V. Sánchez-Pérez[1], S. Castiñeira-Ibáñez[3], L.M. Garcia-Raffi[4]
[1]Centro de tecnologías Físicas: Acústica, Universidad Politécnica de Valencia,
[2]School of Computing, Science & Engineering, University of Salford. Salford, Greater Manchester, M5 4WT, UK
[3]Dpto. Física Aplicada, Universidad Politécnica de Valencia,
[4]Instituto Universitario de Matemática Pura y Aplicada, Universidad Politécnica de Valencia
*Corresponding author: Dpto. Física Aplicada,
Camino de vera s/n
46022, Valencia
Spain.
virogar1@mat.upv.es

Abstract: The elastic and geometrical properties of low density polyethylene (LDPE) foam are used in this paper to improve the attenuation properties of periodic arrangements of acoustic scatterers known as Sonic Crystals (SCs). A specific recycled profile of LDPE foam is used as elastic-acoustic scatterer. The acoustic spectrum of the single scatterer shows two attenuation peaks in the low frequency range. If the elastic scatterers are arranged as a SC, the attenuation spectrum shows the attenuation peaks of the single scatterers at the same position, as well as the attenuation peaks related to the periodicity of the structure.
COMSOL Multiphysics is used to reproduce numerically the frequency response measured experimentally for both the single scatterers and the periodic arrangement. The results provided by COMSOL are in good agreement with the experimental data.

Keywords: Sonic Crystals, Resonant Scatterers, Elastic Scatterers, Phononic Crystals, Band Gap materials.

1. Introduction

Studying periodic distributions of scatterers in a host media has been of increasing interest in recent years [1-12]. The results have been widely adopted in many engineering developments such as photonic crystals [13], phononic crystals [1, 2], sonic crystals [4], wave guides [19] and acoustic filters [11]. Emphasis in these periodic systems has been on achieving large acoustic Band Gaps (BGs), i.e. ranges of frequencies where the wave propagation is forbidden [7-11]. One of the strategies for improving the BGs is to design scatterers with resonant [7] or absorbent behaviours [9].

In the case of the acoustic audible range of frequencies, these periodic distributions of scatterers are called Sonic Crystals (SCs) [4]. In the past few years an increasing interest in the improvement of the attenuation and focusing properties of SC has been studied in the literature. Many developments are based on the modification of the scatterers by adding acoustical properties and the application of optimization algorithms over structures of rigid scatterers.

Genetic Algorithms are widely used to improve the attenuation or focusing properties of the SC made of rigid cylinders. The design of the Quasi-Ordered Structures (QOS) [11] produces new attenuation peaks, and the optimization of the focusing properties of SC can produce new focal points [20].

Introducing the scatterers with added acoustical properties can have different effect on SCs performance. On the one hand, absorbent scatterers [9] can be used to improve the BGs produced by the SCs. On the other hand, resonant scatterers can also be used to introduce new attenuation bands in the SC frequency response [7] that are independent of the periodicity of the array.

In this paper we have analysed experimentally and numerically the acoustical response of recycled scatterers of Low Density Polyethylene (LDPE) Foam. Profiles of this material are used for packing applications, but its geometrical shape and its elastic properties could be exploited as scatterers with added acoustical properties. The experimental data corresponding to the frequency response of the LDPE foam profiles shows two attenuation peaks in the low frequency range. These attenuation properties of the LDPE scatterer may be used for improving the perfomance of SCs. In particular, the frequency response of the periodic arrangement of the LDPE scatterers includes these two new attenuation peaks in the range of low frequencies in addition to the attenuation peaks related with the periodicity of the array.

In this work we have used a numerical model based on COMSOL for modelling the acoustical behaviour of the LDPE scatterers. The geometry shown in figure 1 is used in COMSOL for analysing propagation of sound in the frequency domain. The frequency response is studied for a single scatterer and for a SC with triangular unit cell. The LDPE scatterers are embedded in air and incident plane wave is perpendicular to the axis of the scatterers from the left side. At the boundary of the scatterer the elastic waves are excited by waves of the acoustical field and, reciprocally, vibration of the elastic scatterer contributes to the acoustical field. In this problem the finite element method is a promising alternative to analytical methods because of complex geometry of the LDPE profile.

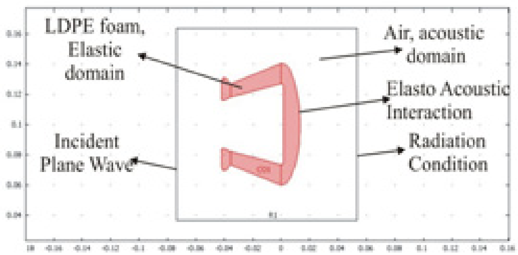

Figure 1. Geometry of the problem. Low density polyethylene foam scatterer (elastic domain) embedded in air (acoustical domain).

The structure of the paper is as follows. In section 2, we show the experimental data obtained for single the LDPE scatterer and for the periodic array of the LDPE scatterers. In Section 3 we show the governing equation of the wave scattering problem, i.e. the elastic-acoustic interaction. The numerical results are shown and discussed in section 4. Finally, we present the conclusions of the work.

2. Experimental results

The experimental data have been measured in an anechoic chamber of size 8x6x3 m^3. We analyzed the well known Insertion Loss: the difference between the sound level measured in a point with and without the sample. The IL provides us the attenuation behavior of the sample.

In this section we show the experimental results for a LDPE scatterer and for periodic array of LDPE scatterers. In figure 2, we can observe a transversal view of the scatterer. This frame is 2 m long and its main material properties are given in the Table 1. Along with the low-density material the frame is characterised by its geometrical shape which could introduce the so-called resonance cavity. We also observe in figure 2 the periodic arrangement, or SC [6], which is based on triangular unit cell whose lattice constant is 12.7 cm.

It must be noted that in this work we are interested in analyzing the specific range of low frequencies. The upper bound of this range corresponds to the first Bragg's frequency corresponding to the lattice constant of 12.7 cm, which is 1545 Hz [6].

Foams are mainly divided in two groups open- and closed-cell. The former can be analysed theoretically as a poroelastic material. However, as Aygun and Attenborough [14] showed, the closed-cell foams cannot be considered as a poroelastic material. The differences in acoustic properties between open- and closed-cell, appear to result from the different cell structures rather than from differences in other physical parameters. On the other hand, Grenestedt [15] has shown analytically and numerically that the mechanical behaviour of the closed-cell polymer foams can be analysed as an effective elastic medium.

Table 1: Physical properties of the low density Polyethylene foam.

	LDPE Foam
Density (kg/m^3)	50
Young's modulus (10^9 Pa)	0.095
Poisson's ratio	0.32

When foam is compressed it exhibits an initial elastic regime which is followed by a plateau regime in which the load required to compress the foam remains nearly constant [16]. We suppose that the LDPE foam belongs to the elastic regime in the range of the acoustic frequencies we are working with. Thus, LDPE foam can be considered as elastic low-density material.

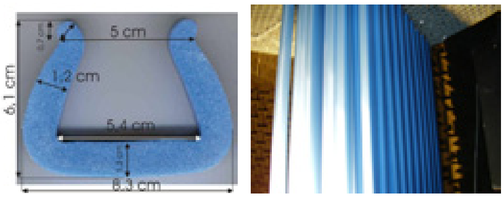

Figure 2. Transversal view of a LDPE foam scatterer. Triangular array of scatterers of lattice constant 12.7 cm.

In Figure 3 is the representation corresponding to the experimental data of the IL for a single LDPE scatterer. In the inset of the figure we can observe the incidence direction and the measurement point. Two attenuation peaks appear before the upper bound of frequencies defined above. The firs peak appears around 700 Hz and the second one around 1100 Hz.

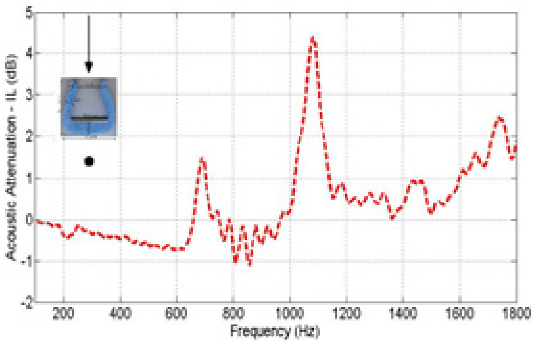

Figure 3. Experimental Insertion Loss of a single scatterer. The incidence direction and the measuring point are shown in the inset.

We have measured the dependence of these attenuation peaks on several parameters, such as the length of the LDPE scatterer and the incidence direction. For these dependences we have observed always the same peaks at the same position. This is experimental evidence that both peaks could be result of a resonant behavior. In fact, the cavity that the LDPE scatterer presents as well as the elastic properties of the material could produce some resonance effect.

In Figure 4 we show the IL corresponding to a periodic arrangement of LDPE scatterers situated in triangular arrangement with lattice constant 12.7 cm in both main directions of symmetry. The receiver positioned on the axis of symmetry is 1 m distant from the last column of SC. Periodic arrangement of 60 LDPE scatterers is arranged in 6 rows of 10 LDPE scatterers. Blue continuous line represents the IL for the 0º of incidence (ΓJ) and red dashed line represents the IL for the case of 30º of incidence (ΓX). Green dot line corresponds to the IL of a single LDPE scatterer.

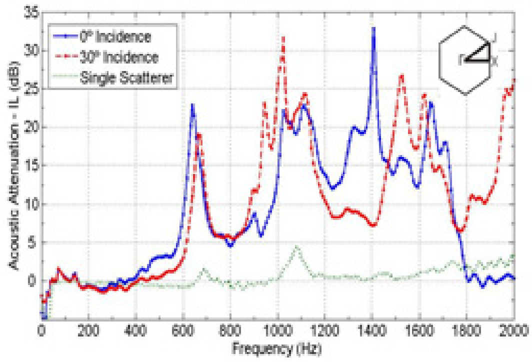

Figure 4. Experimental IL. Blue continuous line represents the IL for the 0º of incidence (ΓJ) and red dashed line represents the IL for the case 30º of incidence (ΓX). Green dot line corresponds to the IL of a single scatterer.

In Figure 4 we observe the attenuation peaks related to the single LDPE scatterer as well as the attenuation peaks related to the periodicity of the array considered. We can observe that the attenuation peaks related to the single LDPE scatterer are independent of the incident wave directions, however, the attenuation peak corresponding to the periodicity depends strongly on the angle of the incident wave. This is perfectly reasonable with the hypothesis that the attenuation peaks of the single LDPE scatterer corresponds to resonance phenomena.

Although the behavior of the attenuation peaks should be explained, this is out of the scope of this paper. In this work we are interested in how COMSOL models the acoustical behavior of a LDPE scatterer with complex geometry. The physics behind each attenuation peak of the spectrum shown in figure 4 will be explained in the reference [18].

3. Elasto-acoustic interaction

In this section we describe the governing equation of the wave scattering problem. We consider the time harmonic case. Suppose we have an elastic medium B embedded in a fluid material A. Then the equation for elastic waves in the medium B is

$$-\rho_B \omega^2 u_i = \left\{ \frac{\partial \sigma_{ij}}{\partial x_j} \right\}, \quad (1)$$

where u_i is the i th component of the displacement vector $\boldsymbol{u(r)}$, ω is the angular frequency and σ_{ij} is the stress-strain relation given by

$$\sigma_{ij} = \lambda_B u_{ll} \delta_{ij} + \mu_B u_{ij},$$

$$u_{ij} = \frac{1}{2}\left(\frac{\partial u_i}{\partial x_j} + \frac{\partial u_j}{\partial x_i} \right).$$

λ_B and μ_B are the so-called Lamé coefficients and ρ_B is the density of the elastic material. The longitudinal and transverse velocities of the material B are given by

$$c_l = \sqrt{\frac{\lambda_B + 2\mu_B}{\rho_B}}, \qquad c_t = \sqrt{\frac{\mu_B}{\rho_B}}, \quad (2)$$

where the Lamé coefficients can be related with the Young's modulus and the Poisson's ratio as usual.

The equation for acoustic waves in the fluid medium A, is

$$-\frac{\omega^2}{c_A^2} p = \nabla \left(\frac{1}{\rho_A} \nabla p \right), \quad (3)$$

where p is the pressure, ρ_A is the density and c_A is the velocity of sound in the medium A.

The solutions of equations (3) and (5) must satisfy the continuity conditions, yielding

$$\left. \frac{\partial p}{\partial n} \right|_{\partial B} = \rho_A \omega^2 \vec{u}\vec{n}, \quad (4)$$

$$\left. \sigma_{ij} n_j \right|_{\partial B} = -p n_i, \quad (5)$$

where ∂B is the boundary of the medium B.

4. Results

A multiphysics model of COMSOL is used to solve the previous elastic-acoustic coupling. A 2D acoustic and plain strain model have been used to solve the frequency response of the system with the appropriated boundary conditions. In the exterior boundaries of the numerical domain the Radiation condition is imposed.

4.1. Single Scatterer

The frequency response of a single LDPE scatterer is shown in Figure 5. The red dashed line represents the experimental data of the IL, and the blue continuous line represents the numerical IL calculated using COMSOL. We can observe both experimentally and numerically two attenuation peaks in the low frequency range. The numerical results show good agreement with the experimental data. The small difference in the attenuation peaks may be result of differences in the geometrical shape implemented in the numerical model.

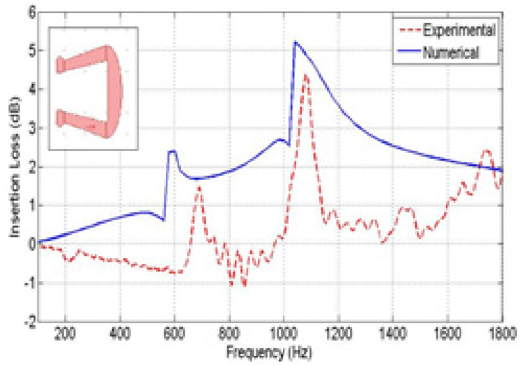

Figure 5. Experimental and Numerical Insertion Loss of a single scatterer of LDPE Foam. Red dashed line represents the experimental IL. Blue continuous line represents the numerical IL.

4.2. Finite periodic arrangement of scatterers

The same finite periodic arrangement used in the experimental set up is reproduced in

COMSOL. We have performed a triangular arrangement of 6 rows of 10 scatters with lattice constant a=12.7 cm. In Figure 6 we can observe the positions of the LDPE scatterers in the interior of the periodic arrangement. Figure 6 and 7 represent two pressure maps corresponding to the frequencies of both attenuation peaks shown in figure 5. Figure 6 corresponds to the map for the frequency of the first attenuation peak, f=600 Hz, whereas figure 7 is the map for the frequency of the second attenuation peak, f=1080Hz. As we have mentioned above the small difference in the attenuation peak at 600 Hz may be result of differences in the geometrical shape implemented in the numerical model. In both figures the incident direction is along the ΓJ direction (0º degrees). In a previous section we have discussed from the experimental spectra that both attenuation peaks observed in the IL spectrum of the single LDPE scatterers, figure 5, may be explained by some resonance phenomena [17]. In Figure 6 as well as in figure 7 we can observe that the maximum values of the acoustic pressure are distributed around the LDPE scatterers, which is a characteristic behavior of resonance effects.

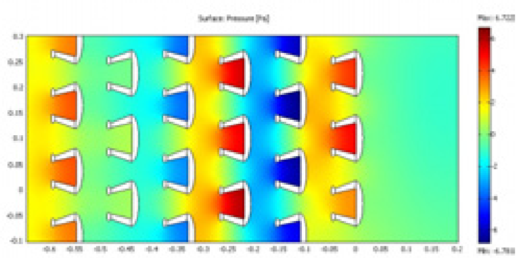

Figure 6. Pressure map in the interior of the finite periodic structure for a plane incident wave of frequency f=600 Hz.

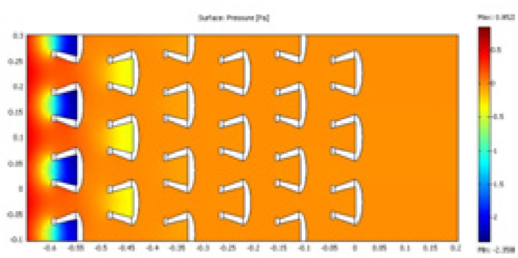

Figure 7. Pressure map in the interior of the finite periodic structure for a plane incident wave of frequency f=1080 Hz.

We have evaluated the IL in a point situated at 1 m from the last row of cylinders and in the axis of symmetry for an incidence of 0º degrees (ΓJ direction). Figure 6 shows the numerical results for such a periodic arrangement. Continuous blue line represents the numerical IL for the triangular arrangement and dashed red line corresponds to the numerical IL for a single LDPE scatterer. The inset zooms the range where the attenuation peaks of the single LDPE scatterer are produced.

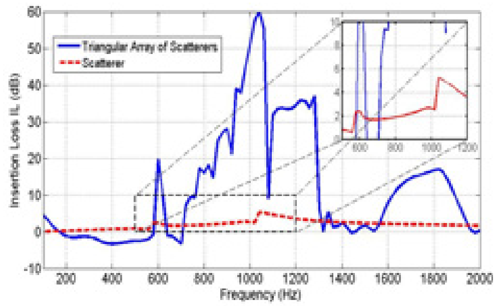

Figure 8. Numerical Insertion Loss. Red line represents the IL of a single scatterer. Blue continuous line represents the IL for a triangular arrangement of LDPE Foam Scatterers with lattice constant a=12.7 cm for the 0º of incidence (ΓJ). Zoom shows the numerical results for a single LDPE scatterer.

5. Conclusion

Scatterers with added acoustical properties are analyzed numerically and experimentally in this work using COMSOL Multiphysics. The results obtained are in good agreement with the experimental ones. Soft scatterers made with LDPE foam with a cavity shows new properties which can improve the acoustical attenuation capability of SC at low frequencies. The LDPE scatterer analyzed in this paper shows two attenuation peaks at low frequencies. These results open new perspective in the design of SC. Several combinations of the LDPE scatterers with different cavities and shapes could be used to attenuate a wide range of frequencies. This can be used in several engineering problems, such as constructing effective acoustic barriers.

6. References

1. Kushwaha, M.; Halevi, P.; Martínez, G.; Dobrzynski, L. & Djafari-Rouhani, B. Theory of

acoustic band structure of periodic elastic composites, *Phys. Rev. B*, **49**, pp. 2313-2322, (1994).

2. Kafesaki, M. & Economou, E. Multiple Scattering theory for three-dimensional periodic acoustic composites, *Phys. Rev. B*, **60**, pp. 11993, (1999).

3. C.M. Linton and P. McIver, Handbook of mathematical techniques for wave/structure interactions, Boca Raton: Chapman & Hall/CRC, (2001).

4. R. Martínez-Sala, J. Sancho, J.V. Sánchez, V. Gómez, J. Llinares and F. Meseguer, Sound Attenuation by sculpture, *Nature*, **378**, pp. 241, (1995).

5. M. Kushwaha, Stop-bands for periodic metallic rods: Sculptures that can filter the noise *Appl. Phys. Lett*., **70**, pp. 3218, (1997).

6. J.V. Sánchez-Pérez, C. Rubio, R. Martínez-Sala, R. Sánchez-Grandia and V. Gómez, Sound Attenuation by a Two-Dimensional Array of Rigid Cylinders, Phys. Rev. Lett. **80 (24),**, pp. 5325, (1998).

7. Z. Liu, X. Zhang, Y. Mao, Y. Zhu, Z. Yang, C. Chan and P.Sheng, Locally Resonant Sonic Materials, *Science*, **289**, pp. 1734, (2000).

8. A.B. Movchan and S. Guenneau, Split-ring resonators and localized modes, *Phys. Rev. B*, **70**, pp. 125116, (2004)

9. O. Umnova K. Attenborough and C.M. Linton, Effects of porous covering on sound attenuation by periodic arrays of cylinders, *J. Acoust. Soc. Am*., **119**, pp. 278-284, (2006).

10. LU TianJian, GAO GuoQin, MA ShouLin, JIN Feng and T. Kim, Acoustic band gaps in two-dimensional square arrays of semi-hollow circular cylinders, *Sci. China Ser. E-Tech Sci*, **52**, pp. 303-312, (2009).

11. V. Romero-García, J.V. Sánchez-Pérez, L.M. Garcia-Raffi, J.M. Herrero, S. García-Nieto, X. Blasco, Hole distribution in phononic crystals: Design and optimization, *J. Acoust. Soc. Am*., **125** (6), pp. 3774-3783, (2009).

12. M. Torres, F.R. Montero de Espinosa, D. García-Pablos and N. Garcia, Sonic Band Gaps in Finite Elastic Media: Surface States and Localization Phenomena in Linear and Point Defects,. *Phys. Rev. Lett*., **82**, 15, pp. 3054-3057, (1999).

13. J. H. Page et al., in Photonic Crystals and Light *Localization in the 21st Century*, edited by C.M. Soukoulis (Kluwer Academic, Amsterdam, 2001)

14. Soukoulis (Kluwer Academic, Amsterdam, 2001), p. 59.

15. H. Aygun and K. Attenborough, Sound absorption by clamped poroelastic plates, *J. Acoust. Soc. Am.*, **124** (3), pp. 1550-1556, (2008).

16. J.L. Grenestedt, Effective elastic behavior of some models for 'perfect' cellular solids, *International Journal of Solids and Structures*, **36**, pp. 1471-1501, (1999).

17. P.F. Soto, M. Herráez, A. González and J.A. de Saja, Acoustic Impedance and Absorption Coefficient Measurements of Porous Materials used in the Automotive Industry, *Polymer Testing*, **13**, pp.77-88, (1994).

18. V. Romero-García, J.V. Sánchez-Pérez, A. Krynkin, L.M. Garcia-Raffi, *The behaviour of sonic crystals made of resonant scatterers.* Proceedings Euronise 2009.

19. A. Khelif, M. wilm, V. Laude, S. Ballandras and B. Djafari-Rouhani, *Guide elastic waves along a rod defect of a two-dimensional phononic crystal,* Phys. Rev. E, 69, 067601, (2004)

20. Hakansson, A.; Dehesa, J. S. and Sanchis, L. *Acoustic lens design by genetic algorithms*, Phys. Rev. B, **2004***, 70*, 214302

7. Acknowledgements

The authors gratefully acknowledge Dr. O. Umnova for her constructive comments. V. Romero-García is grateful to the University of Salford for giving to him the opportunity to develop some results using the university acoustic facilities. This work was supported by MEC (Spanish Government) and FEDER funds, project MAT2009-09438